An approximate decoupled reliability-based design optimization method for efficient design exploration of linear structures under random loads

Lili Weng[a], Cristóbal H. Acevedo[b], Jiashu Yang[c], Marcos A. Valdebenito[b], Matthias G.R. Faes[b], Jianbing Chen[a]

[a] *State Key Laboratory of Disaster Reduction in Civil Engineering & College of Civil Engineering, Tongji University, 1239 Siping Road, Shanghai 200092, China*

[b] *Chair for Reliability Engineering, TU Dortmund University, Leonhard-Euler-Straße 5, Dortmund 44227, Germany*

[c] *School of Civil Engineering, Xi'an University of Architecture and Technology, 13 Yanta Road, Xi'an 710055, China*

Abstract

Reliability-based design optimization (RBDO) provides a promising approach for achieving effective structural designs while explicitly accounting for the effects of uncertainty. However, the computational demands associated with RBDO, often due to its nested loop nature, pose significant challenges, thereby impeding the application of RBDO for decision-making in real-world structural design. To alleviate this issue, an approximate decoupled approach is introduced for a class of RBDO problems involving linear truss structures subjected to random excitations, with the failure event defined by compliance. This contribution aims to provide an approximate but efficient way for design exploration to facilitate decision-making during the initial design phase. Specifically, the proposed approach converts the original RBDO problem into a deterministic optimization problem through a modest number of reliability analyses by the probability density evolution method (PDEM). Once the deterministic optimization problem is obtained, the solution of the whole RBDO problem can be obtained by solving this equivalent problem without further reliability analysis, resulting in notable enhancement in terms of computational efficiency. In this way, this contribution expands the frontier of application of the operator norm theory within the RBDO framework. Numerical examples are conducted to illustrate the effectiveness and capabilities of the proposed approach.

Keywords: Reliability-based design optimization, Decoupling approach, Operator norm theory, Probability density evolution method, Design exploration.

---

1. Introduction

Reliability-based design optimization (RBDO) offers a rational method to attain effective structural designs while ensuring an appropriate level of structural safety. Although RBDO can be advantageous compared with deterministic design procedures in terms of explicitly accounting for the effects of different sources of uncertainty (Valdebenito and Schuëller, 2010; Beck and Gomes, 2012), its application is typically hindered by the high computational cost associated with solving the RBDO problem. In essence, the solution of the RBDO problem involves a double loop procedure, where the outer loop deals with the optimization exploration and the inner loop copes with the reliability evaluation, thus leading to unaffordable numerical efforts.

In this context, numerous effective methods have been proposed to alleviate numerical efforts. These methods can be categorized into three classes: double loop methods, single loop methods and decoupled methods. In the double loop methods, the reliability of each set of design variables explored is estimated throughout the whole optimization process. By means of appropriately integrating optimization algorithms and reliability analysis techniques, higher numerical efficiency can be achieved (Jensen et al., 2009; Carlon et al., 2019; Weng et al., 2023). The single loop methods convert the original double loop problem into a single loop one, by substituting the reliability constraints with approximate deterministic constraints, based on the Karush–Kuhn–Tucker (KKT) optimality conditions associated with the reliability problems (Kuschel and Rackwitz, 1997; Liang et al., 2007; Li et al., 2019). The decoupled methods circumvent double loop implementation by integrating information from reliability analysis into mathematical programming techniques to guide the optimization process. Specifically, the decoupled methods break the original problem down into a series of deterministic optimization cycles, with the corresponding admissible design spaces updated by insights gained from independent reliability analyses. Representative studies include sequential optimization and reliability assessment (SORA) (Du and Chen, 2004; Li et al., 2020) and sequential approximate programming method (SAP) (Cheng et al., 2006; Chen et al., 2020). To further improve the computational efficiency of RBDO, surrogate models have garnered significant attention. These models substitute costly-to-evaluate functions, such as limit state functions, with inexpensive local or global approximations constructed using a modest number of evaluations of the original models (Papadrakakis and Lagaros, 2002; Jensen et al., 2020; Yang et al., 2022c). For a more detailed overview on the RBDO methods, readers are referred to (Schuëller and Jensen, 2008; Valdebenito and Schuëller, 2010; Aoues and Chateauneuf, 2010;

Moustapha and Sudret, 2019; Meng et al., 2020).

Despite the achievements mentioned above, the practical implementation of RBDO remains challenging. Actually, the optimization process in most of the RBDO methods is more or less affected by the reliability analysis, which increases the computational expenses (Faes and Valdebenito, 2020). Moreover, it is noted that most of the above methods were developed in the context of static rather than dynamic problems. To tackle this challenge, Faes and Valdebenito (2020) proposed a fully decoupled approach for a specific class of RBDO problems, aiming to minimize the failure probability of linear systems subjected to random excitations. They subsequently extended this work to the RBDO problems considering discrete design variables (Faes and Valdebenito, 2021). The approach tackles the entire RBDO problem by solving a deterministic problem followed by a single reliability analysis, leading to efficiency improvements of orders of magnitude. Building upon this development, Jiang et al. (2024) further expanded their research to solve the RBDO problems with reliability constraints. By establishing the mapping function between the operator norm and the reliability index using a small number of samples, the original reliability constraint is transformed into a deterministic one with respect to the operator norm, thereby eliminating the nested loop. The theoretical foundation of these contributions rests on the operator norm theory, which has been successfully applied in the realm of imprecise reliability analysis (Muscolino et al., 2016) of both linear systems (Faes et al., 2020, 2021) and nonlinear systems (Ni et al., 2022; Jerez et al., 2024). Specifically, the core is to replace the objective or constraint functions related to reliability by functions defined in terms of the $(\infty, 2)$ matrix norm, which is inherently connected to the definition of the reliability problems (Faes et al., 2021). Despite the proven advantages of applying the operator norm theory, there remains ample opportunity for further exploration and advancement in the field of optimization to fully harness its potential benefits. Additionally, in the aforementioned contributions, structural displacement serves as the metric for defining the failure event. Nonetheless, alternative performance indicators are also of importance and deserve attention. One of such indicators is structural compliance — a typical metric adopted in deterministic topology optimization (Bendsøe and Sigmund, 1999) and robust topology optimization (Chen et al., 2016b; Canelas et al., 2024) of structures.

In this context, this paper proposes an approximate decoupled approach by virtue of the operator norm theory for a specific class of problems, specifically RBDO problems concerning linear truss structures subjected to random excitations with failure event defined by compliance. This contribution extends the application of the operator norm theory within RBDO frameworks and provides an powerful exploratory tool for decision-making in the initial stages of structural design. The core idea of the proposed approach lies in recasting the RBDO problem as a deterministic optimization problem through a few rounds of reliability analyses, based on the interdependency between the reliability index and the operator norm. Once the deterministic optimization problem is determined, the whole RBDO problem can be addressed by solving the deterministic optimization problem without additional reliability analysis. Therefore, the proposed approach is advantageous from a numerical viewpoint. In this contribution, the reliability analysis is conducted by the probability density evolution method (PDEM) (Li and Chen, 2008; Chen and Li, 2009), while the deterministic optimization is carried out by the quantum-inspired particle swarm optimization (QPSO) algorithm (Sun et al., 2004, 2012; Weng et al., 2023). It should be noted that while these methods are chosen based on their demonstrated feasibility, any alternative approaches for both optimization and reliability analysis can be used instead, due to the nature of the underlying problem. The rest of this contribution is organized as follows: Section 2 describes the detailed formulation of the RBDO problem to be solved. Section 3 introduces the approximate decoupled RBDO approach. Several examples are presented to demonstrate the effectiveness of the proposed approach in Section 4. The paper closes with some concluding remarks and the outlook for future research in Section 5.

2. Formulation of the problem

The optimization problems pertinent to this contribution can be stated as:

$$\begin{aligned} \min_{\boldsymbol{x}\in\boldsymbol{\chi}} \quad & f\left(\boldsymbol{x}\right) \\ \text{s.t.} \quad & h_j\left(\boldsymbol{x}\right) \le 0, \quad j = 1, \cdots, n_{\mathrm{h}} \\ & r_k\left(\boldsymbol{x}\right) \le 0, \quad k = 1, \cdots, n_{\mathrm{r}} \\ & \boldsymbol{x} \in \boldsymbol{\chi} \subset \mathbb{R}^{n_x} \end{aligned}, \tag{1}$$

where $\boldsymbol{x} = \left(x_1, \cdots, x_{n_x}\right)^{\mathrm{T}}$ is the n_x-dimensional vector of design variables belonging to an admissible value set $\boldsymbol{\chi} \subset \mathbb{R}^{n_x}$; $f\left(\boldsymbol{x}\right)$ is the objective function; $h_j\left(\boldsymbol{x}\right) \le 0,\ j = 1, \cdots, n_{\mathrm{h}}$ is the set of the standard constraints independent of uncertainty; $r_k\left(\boldsymbol{x}\right) \le 0,\ k = 1, \cdots, n_{\mathrm{r}}$ is the set of the reliability constraints; and $n_x, n_{\mathrm{h}}, n_{\mathrm{r}}$ are the numbers of the design variables, standard constraints, and reliability constraints, respectively.

Generally, the objective function and the standard constraints, e.g., structural mass and construction consumption, are determined by design requirements. The design variables represent some controllable structural properties, such as cross-sectional areas and shape parameters of elements. The reliability constraints are defined in terms of some reliability measure, and thereby ensure structural performance in a probabilistic manner. Typical reliability measures include failure probability and reliability index, leading to reliability constraints defined by

$$r_k\left(\boldsymbol{x}\right) = P_{\mathrm{F},k}\left(\boldsymbol{x}\right) - P_{\mathrm{F},k}^{\mathrm{th}} \leq 0,\ k = 1, \cdots, n_{\mathrm{r}}, \tag{2}$$

or equivalently

$$r_k\left(\boldsymbol{x}\right) = \beta_k^{\mathrm{th}} - \beta_k\left(\boldsymbol{x}\right) \leq 0,\ k = 1, \cdots, n_{\mathrm{r}}, \tag{3}$$

where $P_{\mathrm{F},k}\left(\boldsymbol{x}\right)$ represents the failure probability evaluated at the design $\boldsymbol{x}$ for the kth failure mode; $P_{\mathrm{F},k}^{\mathrm{th}}$ is the predefined threshold of the failure probability for the kth failure mode; β_k^{th} is the threshold of the reliability index for the kth failure mode; and $\beta_k\left(\boldsymbol{x}\right)$ denotes the reliability index corresponding to $P_{\mathrm{F},k}\left(\boldsymbol{x}\right)$ and is calculated by

$$\beta_k\left(\boldsymbol{x}\right) = \Phi^{-1}\left[1 - P_{\mathrm{F},k}\left(\boldsymbol{x}\right)\right], \tag{4}$$

where $\Phi^{-1}\left(\cdot\right)$ is the inverse function of the standard normal cumulative distribution. Consider an n_θ-dimensional vector $\boldsymbol{\Theta} = \left(\Theta_1, \cdots, \Theta_{n_\theta}\right)^{\mathrm{T}} \in \mathbb{R}^{n_\theta}$ of random variables, which is assumed to be exclusively associated with random excitations, following a joint probability density function (PDF) $p_{\boldsymbol{\Theta}}(\boldsymbol{\theta})$. Then the failure probability can be written in terms of a multidimensional integral as

$$P_{\mathrm{F}}\left(\boldsymbol{x}\right) = \Pr\left\{U\left(\boldsymbol{\Theta}; \boldsymbol{x}\right) > 1\right\} = \int_1^\infty p_U(u; \boldsymbol{x})\mathrm{d}u = \int_{u(\boldsymbol{\theta};\boldsymbol{x})>1} p_{\boldsymbol{\Theta}}(\boldsymbol{\theta})\mathrm{d}\boldsymbol{\theta}, \tag{5}$$

where $\Pr\left\{\cdot\right\}$ is the probability operator; $U\left(\boldsymbol{\Theta}; \boldsymbol{x}\right)$ is the normalized response function, whose value is greater than 1 when structural failure occurs, e.g., the response of interest of a system exceeds a prescribed threshold; u is a realization of U; and $\boldsymbol{\theta}$ is a realization of $\boldsymbol{\Theta}$. In addition, the subscript k is omitted for brevity.

Estimating failure probabilities or reliability indices for general structures presents significant challenges from the numerical standpoint, due to the complexity involved in evaluating response functions, which are often analytically intractable. This complexity requires the use of advanced reliability analysis techniques, such as the importance sampling (Au and Beck, 2001a) and the subset simulation (Au and Beck, 2001b), to name a few. Despite their capacity for improved efficiency, these techniques still require numerous re-analyses of structural responses to assess the failure probability. Additionally, their outcomes are prone to noise. These factors pose challenges in solving the RBDO problems, especially with a double loop scheme.

3. Approximate decoupled reliability-based design optimization

As mentioned above, the process of RBDO typically imposes significant computational demands due to its nested double-loop nature. It entails evaluating the failure probabilities within the optimization process for various realizations of design variables, thus requiring numerous repeated structural reliability analyses. Particularly, when each structural analysis in such reliability analysis consumes substantial computational resources, the overall computational expenses associated with RBDO rapidly become prohibitively expensive. In this section, an approximate decoupled approach for addressing the RBDO problems based on the operator norm theory is introduced and elaborated. This approach enables the generation of designs that are slightly conservative, while significantly reducing the number of failure probability evaluations. Therefore, it emerges as a promising tool for facilitating design exploration within RBDO frameworks. Such explorative tools are expecially relevant in early design stages, where the computational expense of 'regular' RBDO procedures might not be justifiable.

3.1. Operator norm of compliance

The operator norm approach proposed by Faes et al. (2020, 2021) concentrates on the problems where the responses of interest can be recast into the following form:

$$\boldsymbol{Y}\left(\boldsymbol{x};\boldsymbol{\Theta}\right)=\boldsymbol{A}\left(\boldsymbol{x}\right)\boldsymbol{\Theta}, \tag{6}$$

where $\boldsymbol{A}\left(\boldsymbol{x}\right):\mathbb{R}^{n_\theta}\mapsto\mathbb{R}^{n_y}$ is a continuous linear map representing the transformation of the uncertain input to the responses of interest, $\boldsymbol{x}\in\boldsymbol{\chi}\subset\mathbb{R}^{n_x}$ is the vector of the design variables, $\boldsymbol{\Theta}\in\mathbb{R}^{n_\theta}$ is the vector of the random variables, and $\boldsymbol{Y}\in\mathbb{R}^{n_y}$ is the vector of structural responses of interest. Examples of such responses are the displacements of either dynamical or static models of linear structures subjected to random loads.

Consider the linear map $\boldsymbol{A}(\boldsymbol{x}) : \mathbb{R}^{n_\theta} \mapsto \mathbb{R}^{n_y}$ between two normed vector spaces $\mathbb{R}^{n_\theta}$ and $\mathbb{R}^{n_y}$ as defined in Eq.(6), and let $\|\cdot\|_{p^{(i)}}$ be a specific $\mathcal{L}_{p^{(i)}}$-norm in these vector spaces with $i \in [1, \infty)$. According to the operator norm theory, there exists a real number $c(\boldsymbol{x}) \in \mathbb{R}$ such that the following inequality always holds for arbitrary vector $\boldsymbol{\Theta} \in \mathbb{R}^{n_\theta}$:

$$\|\boldsymbol{A}(\boldsymbol{x})\,\boldsymbol{\Theta}\|_{p^{(1)}} \leq |c(\boldsymbol{x})| \cdot \|\boldsymbol{\Theta}\|_{p^{(2)}}\,, \tag{7}$$

and hence

$$\|\boldsymbol{Y}(\boldsymbol{x};\boldsymbol{\Theta})\|_{p^{(1)}} \leq |c(\boldsymbol{x})| \cdot \|\boldsymbol{\Theta}\|_{p^{(2)}}\,. \tag{8}$$

These inequalities therefore provide a metric – the operator norm – indicating the maximum extent to which the matrix $\boldsymbol{A}(\boldsymbol{x})$ can stretch the random vector $\boldsymbol{\Theta}$, in terms of a $p^{(1)}$-norm applied to the stretched vector $\boldsymbol{Y}$, relative to a $p^{(2)}$-norm applied to the original vector $\boldsymbol{\Theta}$. Mathematically, it can be expressed as

$$\|\boldsymbol{A}(\boldsymbol{x})\|_{p^{(1)},p^{(2)}} = \inf\left\{c(\boldsymbol{x}) \geq 0 : \|\boldsymbol{A}(\boldsymbol{x})\,\boldsymbol{\Theta}\|_{p^{(1)}} \leq |c(\boldsymbol{x})| \cdot \|\boldsymbol{\Theta}\|_{p^{(2)}}\,, c(\boldsymbol{x}) \in \mathbb{R}, \forall \boldsymbol{\Theta} \in \mathbb{R}^{n_\theta}\right\}, \tag{9}$$

or equivalently,

$$\|\boldsymbol{A}(\boldsymbol{x})\|_{p^{(1)},p^{(2)}} = \sup\left\{\frac{\|\boldsymbol{A}(\boldsymbol{x})\,\boldsymbol{\Theta}\|_{p^{(1)}}}{\|\boldsymbol{\Theta}\|_{p^{(2)}}} : \forall \boldsymbol{\Theta} \in \mathbb{R}^{n_\theta} \text{ with } \boldsymbol{\Theta} \neq \boldsymbol{0}\right\}, \tag{10}$$

where $\inf\{\cdot\}$ and $\sup\{\cdot\}$ denote the infimum and the supremum, respectively; and $\|\cdot\|_{p^{(1)},p^{(2)}}$ represents the operator norm. It is noted that the operator norm $\|\cdot\|_{p^{(1)},p^{(2)}}$ is defined in a deterministic sense and thus irrelevant to the random variables. This property offers significant benefits for design optimization under uncertainties.

In this contribution, a specific type of problems is taken into account: RBDO of static linear truss structures under random loads, with the criterion for structural failure defined in terms of compliance, an inverse metric of the overall stiffness of a structure (Huang and Xie, 2010). Therefore, the failure probability is formulated by:

$$P_{\mathrm{F}}(\boldsymbol{x}) = \Pr\left\{|C(\boldsymbol{\Theta};\boldsymbol{x})\,/c^{\mathrm{th}}| > 1\right\}, \tag{11}$$

where c^{th} is the threshold of the compliance; $C\left(\boldsymbol{\Theta};\boldsymbol{x}\right)$ is the structural compliance defined by

$$C\left(\boldsymbol{\Theta};\boldsymbol{x}\right)=\boldsymbol{F}\left(\boldsymbol{\Theta}\right)^{\mathrm{T}}\boldsymbol{U}\left(\boldsymbol{\Theta};\boldsymbol{x}\right)=\boldsymbol{F}\left(\boldsymbol{\Theta}\right)^{\mathrm{T}}\boldsymbol{K}^{-1}\left(\boldsymbol{x}\right)\boldsymbol{F}\left(\boldsymbol{\Theta}\right). \tag{12}$$

It can also be represented as an inner product, i.e.,

$$C\left(\boldsymbol{\Theta};\boldsymbol{x}\right)=\left|\left\langle\boldsymbol{F}\left(\boldsymbol{\Theta}\right),\boldsymbol{K}^{-1}\left(\boldsymbol{x}\right)\boldsymbol{F}\left(\boldsymbol{\Theta}\right)\right\rangle\right|, \tag{13}$$

where $\boldsymbol{K}^{-1}\left(\boldsymbol{x}\right):\mathbb{R}^m\mapsto\mathbb{R}^m$ is the inverse of the stiffness matrix of the structure; $\boldsymbol{F}\left(\boldsymbol{\Theta}\right)$ and $\boldsymbol{U}\left(\boldsymbol{\Theta};\boldsymbol{x}\right)$ are the m-dimensional vectors of random loads and displacements, respectively, such that $\boldsymbol{U}\left(\boldsymbol{\Theta};\boldsymbol{x}\right)=\boldsymbol{K}^{-1}\left(\boldsymbol{x}\right)\boldsymbol{F}\left(\boldsymbol{\Theta}\right)$. According to the Cauchy–Schwarz inequality, the compliance is bounded by the product of the norms related to each component of the inner product in Eq.(13):

$$C\left(\boldsymbol{\Theta};\boldsymbol{x}\right)=\left|\left\langle\boldsymbol{F}\left(\boldsymbol{\Theta}\right),\boldsymbol{K}^{-1}\left(\boldsymbol{x}\right)\boldsymbol{F}\left(\boldsymbol{\Theta}\right)\right\rangle\right|\leq\left\|\boldsymbol{F}\left(\boldsymbol{\Theta}\right)\right\|_2\cdot\left\|\boldsymbol{K}^{-1}\left(\boldsymbol{x}\right)\boldsymbol{F}\left(\boldsymbol{\Theta}\right)\right\|_2, \tag{14}$$

where $\left\|\boldsymbol{F}\left(\boldsymbol{\Theta}\right)\right\|_2$ is defined as

$$\left\|\boldsymbol{F}\left(\boldsymbol{\Theta}\right)\right\|_2=\left(\sum_{i=1}^{m}\left|f_i\right|^2\right)^{\frac{1}{2}}, \tag{15}$$

with $f_i\in\boldsymbol{F}\left(\boldsymbol{\Theta}\right)$ and $|\cdot|$ denoting the absolute value operator. Note that the second norm on the right-hand side of the inequality in Eq.(14) shares the same form as the left-hand side of the inequality in Eq.(7). By replacing $\boldsymbol{A}\left(\boldsymbol{x}\right)$ with the inverse of the stiffness matrix $\boldsymbol{K}^{-1}\left(\boldsymbol{x}\right)$ of the structure, $\boldsymbol{\Theta}$ with the random loading vector $\boldsymbol{F}\left(\boldsymbol{\Theta}\right)$ acting on the structure , and $p^{(1)}$ with 2, Eq.(7) yields

$$\left\|\boldsymbol{K}^{-1}\left(\boldsymbol{x}\right)\boldsymbol{F}\left(\boldsymbol{\Theta}\right)\right\|_2\leq\left|c\left(\boldsymbol{x}\right)\right|\cdot\left\|\boldsymbol{F}\left(\boldsymbol{\Theta}\right)\right\|_{p^{(2)}}. \tag{16}$$

Then, substituting Eq.(16) into Eq.(14) results in

$$C\left(\boldsymbol{\Theta};\boldsymbol{x}\right)\leq\left\|\boldsymbol{F}\left(\boldsymbol{\Theta}\right)\right\|_2\cdot\left|c\left(\boldsymbol{x}\right)\right|\cdot\left\|\boldsymbol{F}\left(\boldsymbol{\Theta}\right)\right\|_{p^{(2)}}. \tag{17}$$

Therefore, the operator norm can serve as a metric related to the upper bound of the compliance:

$$\left\|\boldsymbol{A}\left(\boldsymbol{x}\right)\right\|_{2,p^{(2)}}=\sup\left\{\frac{\left\|\boldsymbol{K}^{-1}\left(\boldsymbol{x}\right)\boldsymbol{F}\left(\boldsymbol{\Theta}\right)\right\|_2}{\left\|\boldsymbol{F}\left(\boldsymbol{\Theta}\right)\right\|_{p^{(2)}}}:\forall\boldsymbol{F}\left(\boldsymbol{\Theta}\right)\in\mathbb{R}^m\text{ with }\boldsymbol{F}\left(\boldsymbol{\Theta}\right)\neq\boldsymbol{0}\right\}. \tag{18}$$

The calculation of the operator norm in Eq.(10) is evidently contingent upon the selection of the $p^{(1)}$-norm and the $p^{(2)}$-norm, which is highly case dependent. Readers are directed to Faes and Valdebenito (2020) for comprehensive formulations of operator norm with different $p^{(1)}$ and $p^{(2)}$. In the context of calculating the operator norm pertaining to compliance, both $p^{(1)}$ and $p^{(2)}$ are prescribed as 2, which leads to

$$\|\boldsymbol{A}(\boldsymbol{x})\|_{2,2} = \sup\left\{\frac{\|\boldsymbol{K}^{-1}(\boldsymbol{x})\,\boldsymbol{F}(\boldsymbol{\Theta})\|_2}{\|\boldsymbol{F}(\boldsymbol{\Theta})\|_2} : \forall \boldsymbol{F}(\boldsymbol{\Theta}) \in \mathbb{R}^m \text{ with } \boldsymbol{F}(\boldsymbol{\Theta}) \neq \boldsymbol{0}\right\}. \tag{19}$$

As discussed in Tropp (2004), the $(2,2)$ operator norm equals the maximum singular value of the matrix $\boldsymbol{K}^{-1}(\boldsymbol{x})$. The choice of employing an $\mathcal{L}_2$ norm for the numerator stems from the Cauchy–Schwarz inequality, as shown in Eq.(14), while the rationale behind opting for an $\mathcal{L}_2$ norm for the denominator lies in its loose characterization as the energy content of the random load (Faes et al., 2020).

The operator norm (in Eq.(18)), along with Eq.(17), somehow suggests the extend to which the energy within the random load can be amplified towards the compliance. Therefore, it is readily seen that assessing the failure probability defined in Eq.(11) can be approximated by analyzing the operator norm outlined in Eq.(18). This approximation is rooted in the intuition that lower compliance in a global sense corresponds to a reduced failure probability. Moreover, since the calculation of the operator norm is irrelevant to the random variables, such an approximation can significantly reduce the computational costs.

3.2. Transformation of reliability constraint

Based on the developments of Section 3.1, the operator norm correlates with the upper bound of compliance and thus can be used for the approximate analysis of the failure probability. In this contribution, this approximation is adopted within the RBDO framework to replace the reliability constraint by the deterministic constraint on the operator norm defined by Eq.(18). Herein, the reliability index serves as the chosen reliability measure, calculated through the failure probability as depicted in Eq.(4).

To effectively formulate the deterministic constraint function on operator norm, it is crucial to identify the threshold $\mathrm{ON}^{\mathrm{th}}$ of the operator norm corresponding to the specified threshold β^{th} of the reliability index (Jiang et al., 2024). Empirical studies have shown that a direct one-to-one mapping between the operator norm and the reliability index is elusive. To this end, the threshold $\mathrm{ON}^{\mathrm{th}}$ of the operator norm is estimated using the lower segment of a convex hull in the space related to the operator norm and the reliability index, to ensure the feasibility of the solution of the deterministic optimization problem. The convex hull is constructed based on some randomly pre-selected samples of design vectors, whose reliability indexes and operator norms are evaluated ahead of the optimization implementation. This strategy for determining the threshold of the operator norm is justified by the fact that both computational efficiency and design feasibility are crucial considerations in engineering design decision-making. Specifically, the following strategy is employed: firstly, generate n_s samples of design vector $\{\boldsymbol{x}_i\}_{i=1}^{n_s}$ from the design space randomly; then, calculate the reliability indexes $\{\beta_i\}_{i=1}^{n_s}$ and the operator norms $\left\{\|\boldsymbol{A}\|_{2,2}^{i}\right\}_{i=1}^{n_s}$ associated with these design variables; next, construct a convex hull based on the samples $\left\{\left(\beta_i, \|\boldsymbol{A}\|_{2,2}^{i}\right)\right\}_{i=1}^{n_s}$; finally, parameterize the lower segment of the convex hull, which covers the target reliability index β^{th}, with a polynomial function, and estimate the threshold $\mathrm{ON}^{\mathrm{th}}$ of the operator norm corresponding to β^{th} through this polynomial function. Figure 1 provides a visual representation of this strategy. Once the threshold $\mathrm{ON}^{\mathrm{th}}$ is determined, the RBDO problem (Eq.(1)) is transformed into

$$\begin{aligned} \min_{\boldsymbol{x}\in\boldsymbol{\chi}} \quad & f(\boldsymbol{x}) \\ \text{s.t.} \quad & \|\boldsymbol{A}(\boldsymbol{x})\|_{2,2} \leq \mathrm{ON}^{\mathrm{th}} \\ & h_j(\boldsymbol{x}) \leq 0, \qquad j = 1, \cdots, n_{\mathrm{h}} \\ & \boldsymbol{x} \in \boldsymbol{\chi} \subset \mathbb{R}^{n_x} \end{aligned}, \tag{20}$$

and can be tackled without the need for additional reliability analyses. Herein, only one reliability constraint is considered. The utilization of the lower segment of the convex hull to estimate the threshold is justified by its ability to ensure a conservative reliability level of the final design obtained by solving the problem specified in Eq.(20).

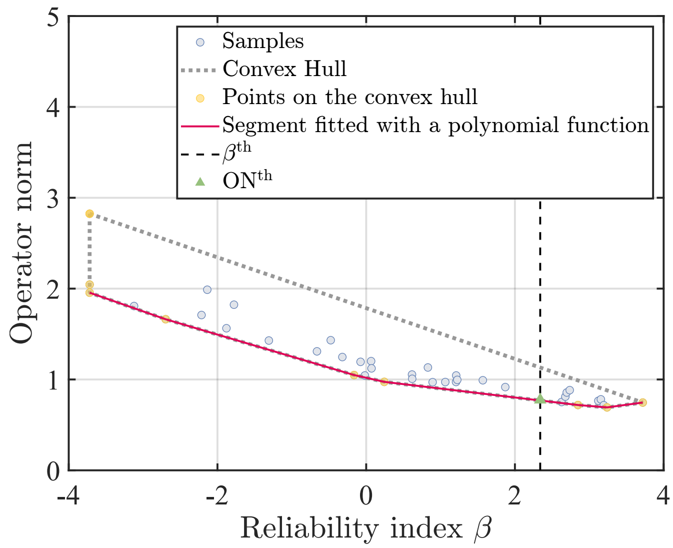

Figure 1: Illustration for identifying the threshold of the operator norm.

However, directly determining the exact threshold ON^{th} of the operator norm may be unfeasible, if the initial number of the random samples is too limited. Moreover, the threshold could be obtained by extrapolating from the limited samples, since the samples may not cover the target reliability index. Therefore, an iterative procedure is adopted to expand the samples for updating the threshold of the operator norm. Specifically, substitute the inaccurate threshold of the operator norm, denoted as $\text{ON}^{\text{th},(1)}$, into Eq.(20), and solve the deterministic optimization problem to obtain a design, denoted as $\boldsymbol{x}_*^{(1)}$. Then, evaluate the reliability index $\beta_*^{(1)}$ and the operator norm $\|\boldsymbol{A}\|_{2,2}^{*(1)}$ of the design $\boldsymbol{x}_*^{(1)}$. If the reliability index is smaller than the target reliability index, namely $\beta_*^{(1)} < \beta^{\text{th}}$, insert the point $\left(\beta_*^{(1)}, \|\boldsymbol{A}\|_{2,2}^{*(1)}\right)$ to the set $\left\{\left(\beta_i, \|\boldsymbol{A}\|_{2,2}^{i}\right)\right\}_{i=1}^{n_s}$, and implement the same strategy mentioned above to obtain an updated threshold $\text{ON}^{\text{th},(2)}$. The threshold is repeatedly updated until a proper threshold $\text{ON}^{\text{th},(l)}$ $(l \geq 1)$ is found, such that $\beta_*^{(l)} > \beta^{\text{th}}$ is satisfied. Since $\text{ON}^{\text{th},(l)}$ can typically be obtained after a few iterations, the numerical costs are not expected to increase significantly.

It should be noted that this strategy tends to produce slightly conservative optimization solutions, although not consistently so. Moreover, the construction of the convex hull can be influenced by the randomly pre-selected design samples, which consequently affects the level of conservatism of the optimization results. Nonetheless, the optimization results are always feasible. It is also noted that reliability analysis is only required for estimating and updating the threshold of the operator norm, as well as for calculating the reliability index of the final design. This approach, therefore, can significantly enhance computational efficiency of RBDO.

3.3. Reliability analysis

While the proposed approach significantly reduces the number of reliability analyses, further efficiency gains can be achieved with the utilization of a general analysis method. In this context, the probability density evolution method (PDEM) is adopted (Chen and Li, 2009). The PDEM stands as a theoretically rigorous and universally applicable approach for analyzing structural stochastic responses (Cao et al., 2023). Its effectiveness in design optimization under uncertainties has been verified in prior research (Yang et al., 2022a,b), demonstrating its status as a powerful tool in the realm of RBDO.

The theoretical foundation of the PDEM is rooted in the stochastic event description of the principle of preservation of probability (Chen and Li, 2009). From this standpoint, a partial differential equation known as the generalized density evolution equation (GDEE), which governs the evolution of the PDF of the structural response of interest, can be derived (Li and Chen, 2008). If only one stochastic response is considered, the GDEE is reduced to a one-dimensional partial differential equation. For the reliability analysis of the structure, the PDEM should be combined with either the absorbing boundary condition approach (Li and Chen, 2005) or the extreme value distribution approach (Chen and Li, 2007). The absorbing boundary condition approach favors time-dependent reliability problems, which are outside the scope of this contribution. Hence, the extreme value distribution approach is adopted.

According to the extreme value distribution approach, the structural reliability could be evaluated by integrating the PDF of an equivalent extreme-value random variable associated with structural failure events. Since the failure events are defined by structural compliance herein, the equivalent extreme-value random variable essentially represents the compliance. Therefore, the problem of reliability analysis is transferred to the solution of the PDF of the compliance. This can be readily achieved through the PDEM.

Specifically, construct a virtual stochastic process associated with the normalized compliance, namely

$$W\left(\boldsymbol{\Theta}, \tau; \boldsymbol{x}\right) = U\left(\boldsymbol{\Theta}; \boldsymbol{x}\right) \cdot \sin\left(\omega_c \tau\right), \tag{21}$$

which satisfies

$$W\left(\boldsymbol{\Theta}, \tau; \boldsymbol{x}\right)\big|_{\tau=0} = 0, \tag{22}$$

$$W\left(\boldsymbol{\Theta}, \tau; \boldsymbol{x}\right)\big|_{\tau=\tau_c} = U\left(\boldsymbol{\Theta}; \boldsymbol{x}\right), \tag{23}$$

where $U(\boldsymbol{\Theta}; \boldsymbol{x})$ denotes the normalized compliance, that is $|C(\boldsymbol{\Theta}; \boldsymbol{x}) / c^{\text{th}}|$ in Eq.(11); τ represents the virtual time; ω_c and τ_c are the parameters of the virtual process, specified as 2.5π and 1, respectively.

Then, the GDEE corresponding to the virtual stochastic process takes the following form:

$$\frac{\partial p_{W\boldsymbol{\Theta}}(w, \boldsymbol{\theta}, \tau; \boldsymbol{x})}{\partial \tau} + \dot{W}(\boldsymbol{\theta}, \tau; \boldsymbol{x}) \frac{\partial p_{W\boldsymbol{\Theta}}(w, \boldsymbol{\theta}, \tau; \boldsymbol{x})}{\partial w} = 0 \tag{24}$$

whose initial condition is

$$p_{W\boldsymbol{\Theta}}(w, \boldsymbol{\theta}, \tau; \boldsymbol{x})|_{\tau=0} = \delta(w) \, p_{\boldsymbol{\Theta}}(\boldsymbol{\theta}), \tag{25}$$

where $p_{W\boldsymbol{\Theta}}(w, \boldsymbol{\theta}, \tau; \boldsymbol{x})$ is the joint PDF of $(\boldsymbol{W}, \boldsymbol{\Theta})$; $\dot{W}(\boldsymbol{\theta}, \tau; \boldsymbol{x})$ is the velocity process of the virtual stochastic process; and $\delta(\cdot)$ is Dirac's delta function. This initial-value problem can be solved by different numerical procedures, and the finite difference method (FDM) with the total variation diminishing (TVD) scheme is adopted (Chen et al., 2020).

After solving the GDEE, one can get the PDF of the normalized compliance $p_U(u; \boldsymbol{x})$ by calculating the marginal distribution:

$$p_U(u; \boldsymbol{x}) = \int_{\Omega_{\boldsymbol{\Theta}}} p_{W\boldsymbol{\Theta}}(w, \boldsymbol{\theta}, \tau; \boldsymbol{x}) \mathrm{d}\boldsymbol{\theta} \bigg|_{w=u, \tau=\tau_c}. \tag{26}$$

Finally, the failure probability and the corresponding reliability index of the structure can be calculated through Eq.(5) and Eq.(4), respectively. Readers are referred to Li and Chen (2009) for more technical details. For completeness, the numerical procedures implemented in this contribution are outlined in the Appendix.

3.4. Optimization

For solving the deterministic problem presented in Eq.(20), any appropriate algorithms can be adopted. In this contribution, the quantum particle swarm optimization (QPSO) algorithm (Sun et al., 2004) is utilized. Renowned as a novel optimization algorithm incorporating quantum mechanics theories, the QPSO and its variants have been extensively adopted to address various optimization problems (dos Santos Coelho, 2010; Agrawal et al., 2021). By leveraging the characteristics of quantum states to enhance particle movements within the search space, QPSO distinguishes itself from canonical particle swarm optimization (PSO), and exhibits superior convergence speed and robustness (Weng et al., 2023).

In the PSO, the movement of particles relies on both their positions and velocities, where the positions represent a collection of potential solutions to the optimization problem (Kennedy and Eberhart, 1995; Meng et al., 2020). In contrast, the QPSO describes the position of a particle probabilistically using a wave function, with its square representing the PDF of the position. Moreover, the QPSO assumes that the wave function adopts the same form as that associated with a real physical particle in a Delta potential well. Therefore, the wave function can be yielded by solving the corresponding time-independent Schrödinger equation. Based on the wave function, the particle's position can be updated by using Monte Carlo simulation.

For practical implementation, the positions of the particles are updated by the following equation:

$$x_j^{(i,\ell+1)} = \eta_j^{(i,\ell)} \pm \frac{L_j^{(i,\ell)}}{2} \ln\left(1/u_j^{(i,\ell)}\right), j = 1, \cdots, n_x, \tag{27}$$

where $x_j^{(i,\ell+1)}$ denotes the jth component of the ith particle's position at the $(\ell+1)$th optimization step; $\eta_j^{(i,\ell)}$ is the local attractor of the particle's position component, given by

$$\eta_j^{(i,\ell)} = \frac{\varphi_j^{(i,\ell)}\ \mathrm{pb}_j^{(i,\ell)} + \phi_j^{(i,\ell)}\ \mathrm{gb}_j^{(\ell)}}{\varphi_j^{(i,\ell)} + \phi_j^{(i,\ell)}}; \tag{28}$$

$L_j^{(i,\ell)}$ is the characteristic length defined by

$$L_j^{(i,\ell)} = 2\alpha \cdot \left|x_j^{(i,\ell)} - \eta_j^{(i,\ell)}\right|; \tag{29}$$

$u_j^{(i,\ell)}, \varphi_j^{(i,\ell)}, \phi_j^{(i,\ell)}$ are random numbers sampled from a uniform distribution within the range $[0,1]$; $\mathrm{pb}_j^{(i,\ell)}$ is the jth component of the ith particle's optimal position; $\mathrm{gb}_j^{(\ell)}$ is the jth component of the global best position of the particle swarm; and α denotes the contraction–expansion coefficient, which regulates the convergence rates of particles. The selection of the contraction–expansion coefficient α can be referred to Sun et al. (2012). Additionally, to cope with the constraints of the optimization problem, a penalty-based method is employed to transform the constrained optimization problem into an unconstrained one (Weng et al., 2023), which is subsequently solved by the QPSO introduced in this section.

3.5. Summary of the proposed approach

The proposed approach for RBDO of a linear truss structure subjected to random loads can be summarized as follows:

1. Formulate the RBDO problem to be solved into the form presented in Eq.(1).
2. Determine the threshold of the operator norm and formulate the deterministic optimization problem, as illustrated in Section 3.2, i.e.,
   a) Generate a limited number of samples of the design vector from the design space, calculate their operator norms, and evaluate their reliability indexes with the PDEM introduced in Section 3.3.
   b) Evaluate the threshold of the operator norm corresponding to the target reliability index, by fitting the lower segment of the convex hull with polynomials.
   c) Transform the RBDO problem (Eq.(1)) into a deterministic optimization problem (Eq.(20)) based on the threshold of the operator norm.
   d) Solve the deterministic optimization problem using the QPSO introduced in Section 3.4.
   e) Update the threshold of the operator norm iteratively. Specifically, assess the reliability level of the final design of the deterministic optimization problem in Step 2.c). If the reliability constraint in Eq.(1) is satisfied at the final design, terminate the iteration and go to Step 3. Otherwise, return to step 2.b) to update the threshold of the operator norm, while considering the reliability index and operator norm associated with the last final design.
3. Output the final results in Step 2 and terminate the whole algorithm.

4. Numerical examples

In this section, four numerical examples are conducted to demonstrate the effectiveness and efficiency of the proposed approach. Two termination criteria for the optimization process are adopted: (1) reaching the maximum number of reliability function calls; (2) reaching the maximum number of iteration N_{It}. The first example aims primarily to validate the effectiveness of the proposed approach. Therefore, only the second termination criterion is employed to ensure a thorough search of the design space.

4.1. Test example: Shape optimization of a 5-bar linear truss structure

The first example focuses on the shape optimization of a 5-bar linear truss structure, as shown in Figure 2. The truss is simply supported on the left side and subjected to a random Gaussian load modelled as a random variable. The mean value and coefficient of variation of the Gaussian load are assumed to be 44.4822 kN and 0.15, respectively. The structural parameters are set as:

the mass density $\rho = 2.768 \times 10^{-6}$ kg/mm^3, and the modulus of elasticity $E = 68947.573$ MPa, the cross-sectional areas of all the bars $A_i = 645.16$ mm^2 $(i = 1, \cdots, 5)$.

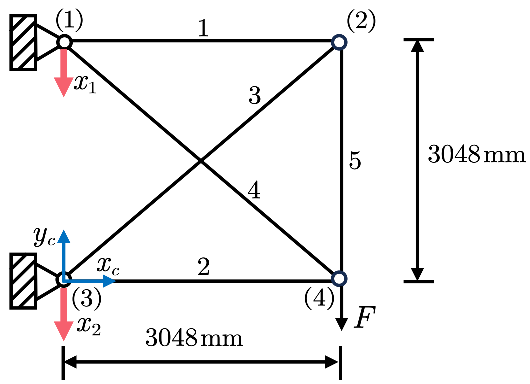

Figure 2: A 5-bar truss structure (Test example).

The objective of the design optimization is to minimize the total mass of the truss structure, while ensuring that the reliability index of the structure remains higher than $\beta^{\text{th}} = 2.34$, (i.e., $P_{\text{F}}^{\text{th}} = 0.01$). The structure is considered to be failed if structural compliance exceeds the prescribed threshold of the compliance, $c^{\text{th}} = 4$ ($\times 112.984$ kN $\cdot$ mm). The design vector $\boldsymbol{x} = (x_1, x_2)^{\text{T}} (\times 25.4 \text{ mm})$ represents the vertical coordinates of the structural supports. Therefore, the optimization problem is formulated as:

$$\begin{array}{cc} \min\limits_{x_1, x_2} & \sum_{i=1}^{5} A_i l_i \left(x_1, x_2\right) \rho \\ \text{s.t.} & 2.34 - \beta\left(x_1, x_2\right) \leq 0 \\ & x_1 \in [60, 140] \\ & x_2 \in [-20, 60] \end{array}, \tag{30}$$

where l_i is the length of the ith bar.

For comparison, the RBDO problem is solved by both a double loop approach and the proposed approach, with a brute-force search scheme: that is, the solution of the optimization problems (both the original RBDO problem and the corresponding deterministic optimization problem) are obtained by finding the optimal designs among a large number of designs generated randomly. To this end, a total of 10000 sets of design variables are randomly generated. The double loop approach utilizes the PDEM to evaluate the reliability index for each realization of the design vector during the optimization process. The reliability index of the structure is calculated with 100 representative points.

Figure 3 presents the operator norm as a function of the reliability index. It illustrates a discernible overall trend wherein the reliability index exhibits an increase as the operator norm decreases. To demonstrate the effectiveness of the proposed approach, 20 samples of the design variables are considered initially to evaluate the threshold of the operator norm, yielding the threshold $\mathrm{ON}^{\mathrm{th}}$ of 0.041, as shown in Figure 4. The contours of the operator norm and the reliability index are depicted in Figure 5, along with the feasible domains for both approaches. It is observed in Figure 5 that the feasible domains of the two approaches are close to each other, which makes it appropriate to replace the original RBDO problem with the deterministic problem. Table 1 presents the final results obtained by both brute-force search with 10000 designs. The results reveal that the proposed approach yields a slightly conservative design, showcasing its feasibility for design optimization under uncertainty. Additionally, in the case of the double loop approach, exploration of the feasible domain necessitates assistance from reliability analysis. However, for the proposed approach, only the calculation of the deterministic operator norm is required to explore the feasible domain, which thereby enhances optimization efficiency.

The RBDO problem is also solved by the QPSO algorithm introduced in Section 3.4. The population size N_{p} and the maximum number of iteration N_{It} are set as 30 and 100, respectively. Table 2 presents the final results obtained by the QPSO optimizer. It demonstrates the feasibility of the proposed approach for generating effective designs. Figure 6 shows the failure probability curve evaluated at the final design of the proposed approach (see Table 2) by the PDEM with 100 representative points and by Monte Carlo simulation (MCS) with 10000 samples. It is seen that the curve obtained by the PDEM is in accord with that obtained by MCS, demonstrating the effectiveness of the PDEM in terms of the reliability analysis.

Table 1: The results obtained by brute-force search within 10000 designs (Test example).

Approach	Threshold	Objective function value	Operator norm	β	x_1	x_2
Double loop approach	$\beta^{\mathrm{th}} = 2.34$	70.956	0.042	2.360	121.898	-11.400
Operator norm-based approach	$\mathrm{ON}^{\mathrm{th}} = 0.041$	71.053	0.041	2.365	128.658	-6.168

Note: the unit of the objective function value is ($\times$ 0.4536 kg); the unit of the design variables $x_i,\ i = 1, 2$, is ($\times$ 25.4 mm).

Table 2: The results obtained by the QPSO optimizer (Test example).

Approach	Threshold	Objective function value	Operator norm	β	x_1	x_2
Double loop approach	$\beta^{\mathrm{th}} = 2.34$	70.922	0.043	2.326	118.794	-13.617
Proposed approach	$\mathrm{ON}^{\mathrm{th}} = 0.041$	71.038	0.041	2.366	128.056	-6.605

Note: the unit of the objective function value is ($\times$ 0.4536 kg); the unit of the design variables $x_i,\ i = 1, 2$, is ($\times$ 25.4 mm).

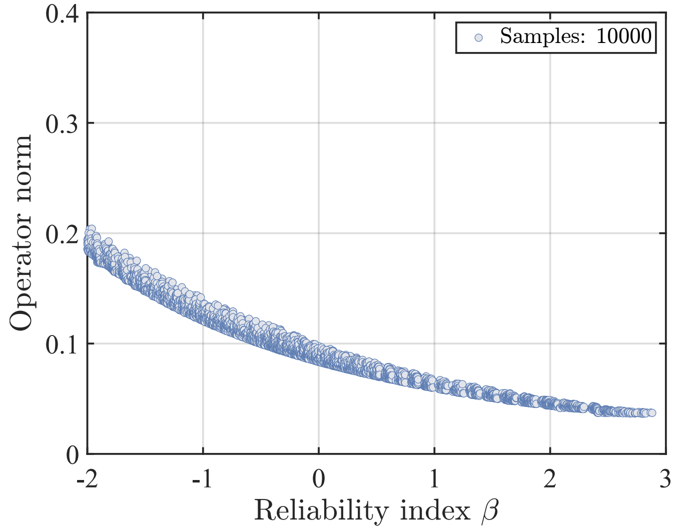

Figure 3: Reliability index versus operator norm (Test example).

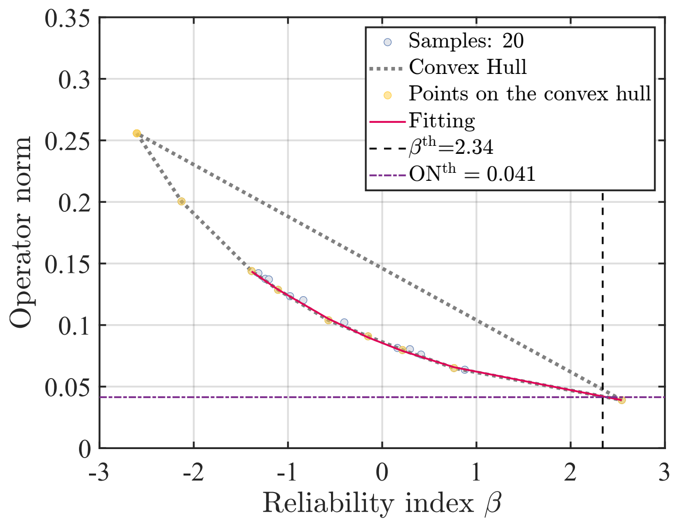

Figure 4: The evaluation of the threshold of the operator norm (Test example).

4.2. Application 1: Size optimization of a 15-bar linear truss structure

The second example involves the size optimization of a 15-bar linear truss structure illustrated in Figure 7. The structure is subjected to a random Gaussian load with the mean value of 44.4822 kN and the coefficient of variation of 0.15. The structural parameters are the same as those of Test example, including the mass density and the modulus of elasticity.

The design optimization aims at minimizing structural mass under a constraint on the reliability index of the structure. The threshold of the compliance for defining failure event is set as 50 ($\times$112.984 kN $\cdot$ mm). The design variables are the cross-sectional areas of the 15 bars, all of which belong to the interval [0.001, 2] ($\times$645.16 mm^2). The design optimization problem is

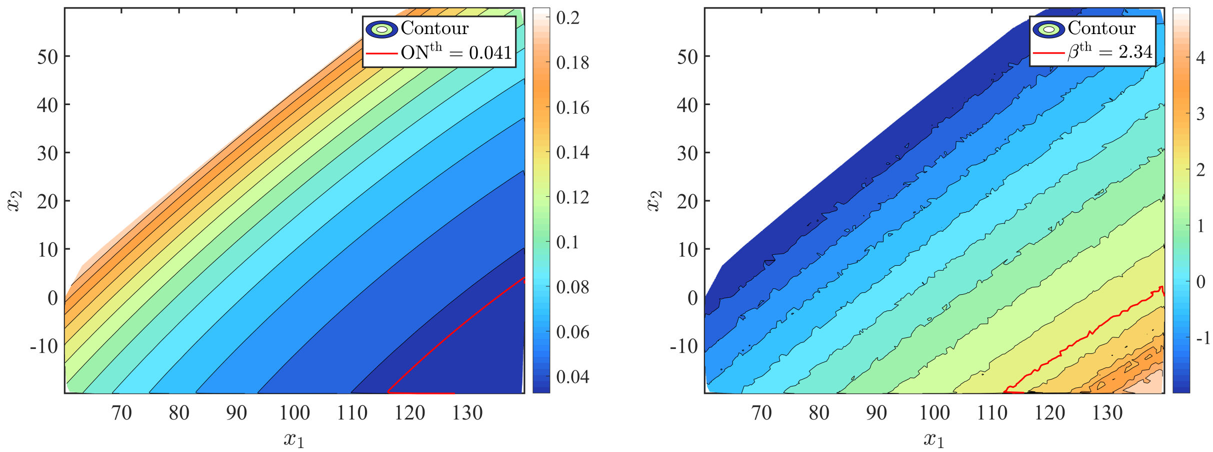

(a) Operator norm (b) Reliability index

Figure 5: The contours of the operator norm and the reliability index (Test example). (The regions in the lower right part of the red contour lines represent the feasible domains; the units of the design variables x_1 and x_2 are ($\times$ 25.4 mm).)

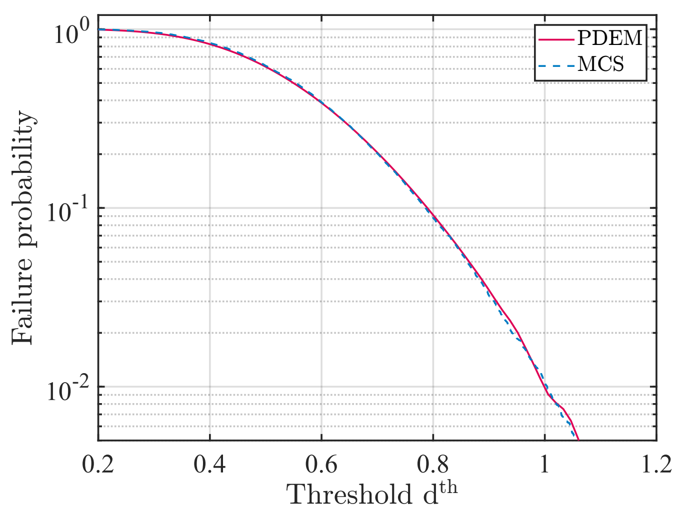

Figure 6: Probability failure curve obtained by the PDEM and MCS (Test example).

formulated as

$$\begin{array}{ccc} \min\limits_{\boldsymbol{x}=(x_1,\cdots,x_{15})^{\mathrm{T}}} & \sum_{i=1}^{15} x_i l_i \rho & \\ \text{s.t.} & 2.34-\beta\left(\boldsymbol{x}\right)\leq 0 & . \\ & x_i \in [0.001, 2], i=1,\cdots,15 & \end{array} \tag{31}$$

The optimization problem is also solved by both the double loop approach and the proposed approach. For both approaches, the reliability index of the structure is estimated through the PDEM with 200 representative points; the population size N_{p} is 30; and the maximum number

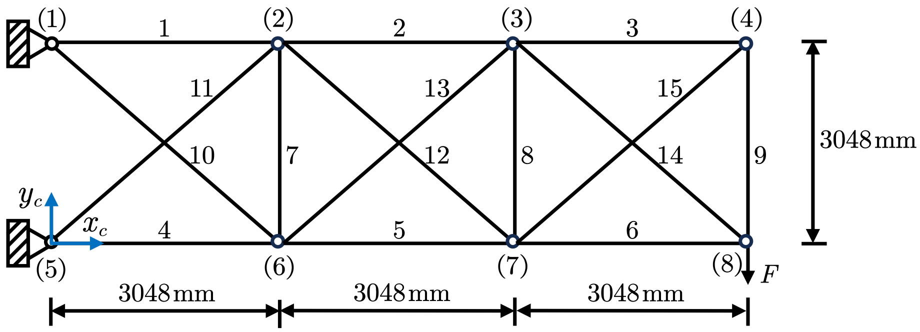

Figure 7: A 15-bar truss structure (Application 1).

of iteration N_{It} is 300. Initially, the threshold of the operator norm is evaluated with 50 samples of the design vector. For updating the threshold of the operator norm, additional 4 rounds of reliability analysis are required, as shown in Figure 8.

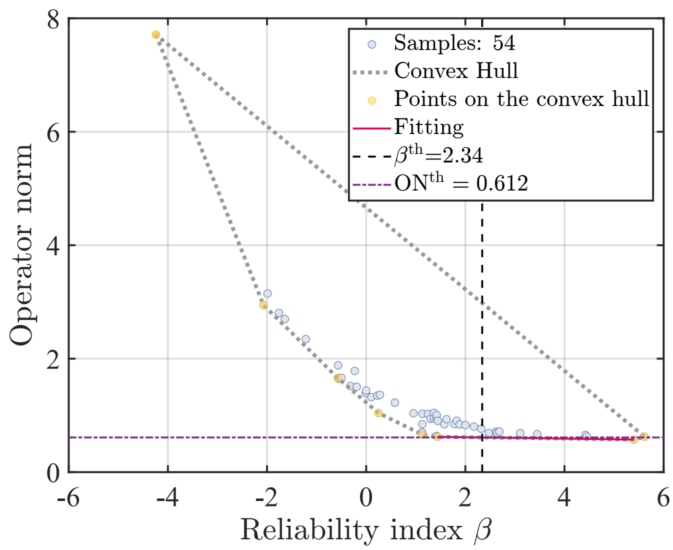

Figure 8: The evaluation of the threshold of the operator norm (Application 1).

Figure 9 shows the the operator norms and failure probabilities associated with 10000 randomly selected design variables, revealing a trend that the reliability index increases as the operator norm decreases. The objective function values and the corresponding design variables resulting from the proposed approach and the double loop approach are presented in Tables 3-4. The optimization termination criterion stipulates a maximum of 1000 calls to the reliability function. The results show that the proposed approach allows for the generation of a design whose objective function value is comparable to that obtained by using the double loop approach, but at a greatly lower computational cost, with the number of function evaluations reduced by an order of magnitude.

It is important to note that for calculating the number of function evaluations for the proposed approach, the number of operator norm evaluations involved in solving the deterministic optimization problem is considered, due to the necessity to evaluate the inversion of the stiffness matrix. The number of operator norm evaluations is associated with the selection of the optimizer for solving the deterministic optimization problem.

It should also be noted that a better result may be obtained by continuing the optimization process for the double loop approach. For example, if the maximum number of iteration $N_{\text{It}} = 300$ is reached, the double loop approach can yield a design whose objective function value and operator norm are 132.708 ($\times$ 0.4536 kg) and 0.790, respectively. However, achieving a 12.2% improvement in the objective function value compared to that obtained by the proposed approach (see Table 3) entails a substantial computational cost, necessitating 9000 rounds of reliability analyses. For the preliminary phases of engineering projects, engineers usually prioritize efficiency and computational feasibility. In this context, the approach proposed in this paper emerges as an effective tool, offering the ability to achieve competitive design outcomes with significantly reduced computational burdens.

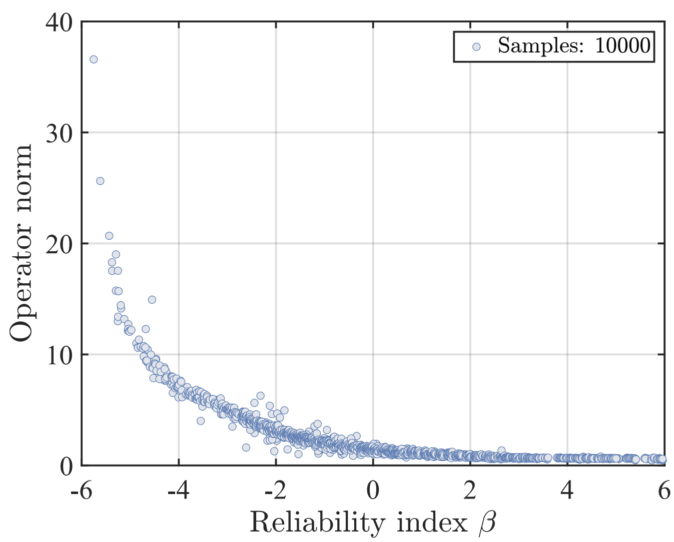

Figure 9: Reliability index versus operator norm (Application 1).

4.3. Application 2: Size and shape optimization of a 15-bar linear truss structure

4.3.1. Case 1: A single random load

The third example involves the size and shape optimization of the 15-bar linear truss structure illustrated in Figure 7. The load condition and the structural parameters are the same as those

Table 3: The results obtained by different approaches (Application 1).

Approach	Threshold	N_r	N_f	Objective function value	Operator norm	β
Double loop approach	β^{th} =2.34	990	198000	147.876	0.790	2.409
Proposed approach	$\mathrm{ON}^{\mathrm{th}}$=0.612	54+1	20000	148.938	0.612	2.409

Note: (1) N_r and N_f denote the numbers of reliability analyses and function evaluations; (2) the unit of the objective function value is (× 0.4536 kg).

Table 4: The design variables obtained by different approaches (Application 1).

Approach	x_1	x_2	x_3	x_4	x_5	x_6	x_7	x_8
Double loop approach	1.409	1.057	0.725	1.152	1.250	0.149	0.001	0.092
Proposed approach	1.996	1.066	0.414	1.976	1.265	0.308	0.006	0.001
Approach	x_9	x_{10}	x_{11}	x_{12}	x_{13}	x_{14}	x_{15}	
Double loop approach	0.857	0.059	1.076	1.407	0.153	0.300	0.987	
Proposed approach	0.070	0.708	0.842	0.780	0.539	0.348	0.538	

Note: the unit of the design variables x_i, $i = 1, \cdots, 15$, is $(\times 645.16 \text{ mm}^2)$.

of Application 1. The objective of this problem is to minimize structural mass under a reliability constraint. The threshold of the compliance is taken as 50 $(\times 112.984 \text{ kN} \cdot \text{mm})$. The design variables are comprised of the cross-sectional areas a_i $(\times 645.16 \text{ mm}^2), i = 1, \cdots, 15$, and part of the nodes' coordinates, namely $\boldsymbol{x}_c = (x_{c2}, x_{c3}, y_{c2}, y_{c3}, y_{c4}, y_{c6}, y_{c7}, y_{c8})^{\mathrm{T}}$ $(\times 25.4 \text{ mm})$ (Ho-Huu et al., 2015). Therefore, the RBDO problem to be solved is

$$
\begin{aligned}
\min_{\boldsymbol{x}=(a_1,\cdots,y_{c8})^{\mathrm{T}}} \quad & \textstyle\sum_{i=1}^{15} a_i l_i(\boldsymbol{x}_c)\,\rho \\
\text{s.t.} \quad & 2.34 - \beta(\boldsymbol{x}) \leq 0 \\
& a_i \in [0.001, 2], i = 1, \cdots, 15 \\
& x_{c2} = x_{c6} \\
& x_{c3} = x_{c7} \\
& 100 \leq x_{c2}, y_{c2}, y_{c3} \leq 140 \\
& 220 \leq x_{c3} \leq 260 \\
& 50 \leq y_{c4} \leq 90 \\
& -20 \leq y_{c6}, y_{c7} \leq 20 \\
& 20 \leq y_{c8} \leq 60
\end{aligned}
\quad . \tag{32}
$$

The problem is solved by both the double loop approach and the proposed approach, with identical settings described in Application 1, except for the population size N_p set as 50 and the maximum number of iteration N_{It} set as 500.

Figure 10 illustrates the values of the operator norm and failure probability associated with 10000 design variables. The figure shows a trend similar to that observed in Application 1, i.e., the increase in the operator norm comes with the decrease in the reliability index. For the proposed approach, the threshold of the operator norm is evaluated with only 50 rounds of reliability analyses, as shown in Figure 11. Table 5 presents the results obtained by both the proposed approach and the double loop approach, wherein a maximum of 2000 calls to the reliability function are restrained. The corresponding designs are shown in Figures 12-13.

It is seen that the proposed approach can generate a design comparable to that of the double loop approach in terms of the objective function value, while significantly reducing the computational costs. When the maximum number of iteration $N_{\mathrm{It}} = 500$ is reached, the double loop approach can produce an improved design, as shown in Figure 14, with the objective function value of 108.364 ($\times$ 0.4536 kg) and the operator norm of 0.837. Nonetheless, such a 5.5% improvement in the objective function value, compared to those in Table 5, demands considerable computational expense. Specifically, 25,000 rounds of reliability analyses are required to achieve this improvement. Given this, the proposed approach can efficiently deliver competitive design outcomes under limited computational resources, which is therefore advantageous in the preliminary phases of engineering design.

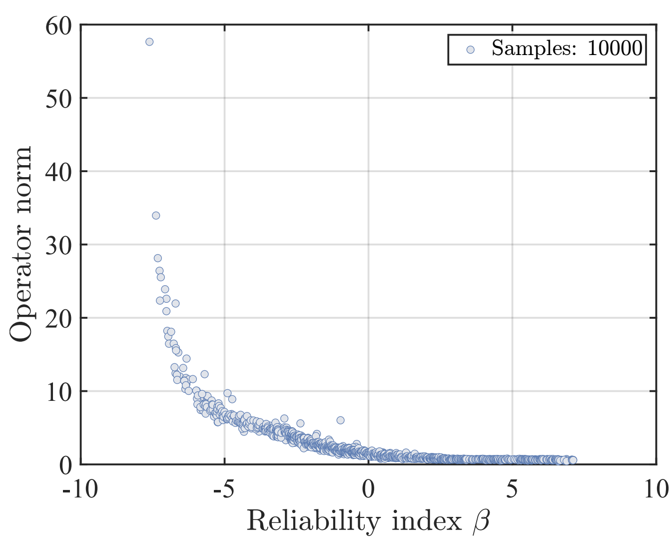

Figure 10: Reliability index versus operator norm (Application2: Case 1).

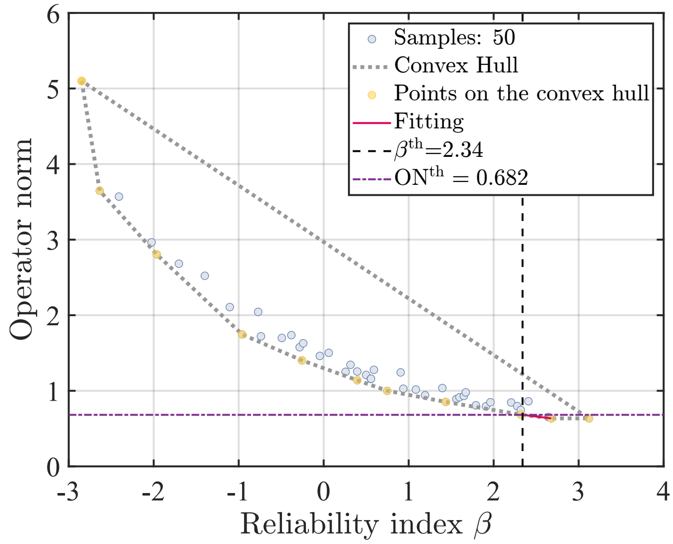

Figure 11: The evaluation of the threshold of the operator norm (Application2: Case 1).

Table 5: The results obtained by different approaches (Application2: Case 1).

Approach	Threshold	N_r	N_f	Objective function value	Operator norm	β
Double loop approach	β^{th} =2.34	2000	400000	115.024	0.828	2.409
Proposed approach	ON^{th}=0.682	50+1	35200	114.346	0.682	2.366

Note: (1) N_r and N_f denote the numbers of reliability analyses and function evaluations; (2) the unit of the objective function value is (× 0.4536 kg).

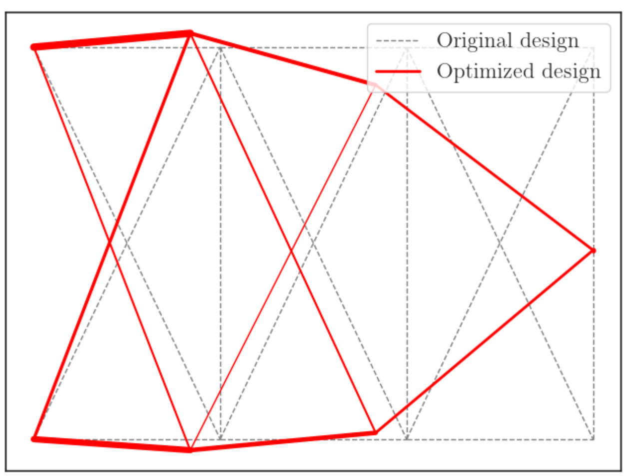

Figure 12: The final truss structure obtained by the proposed approach (Application2: Case 1).

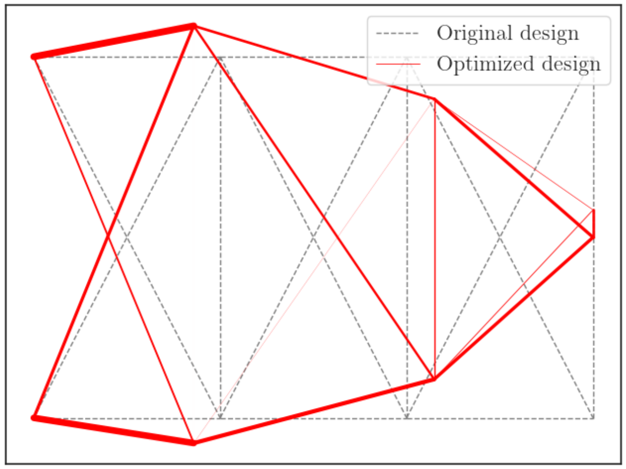

Figure 13: The final truss structure obtained by the double loop approach at 40th optimization iteration (Application2: Case 1).

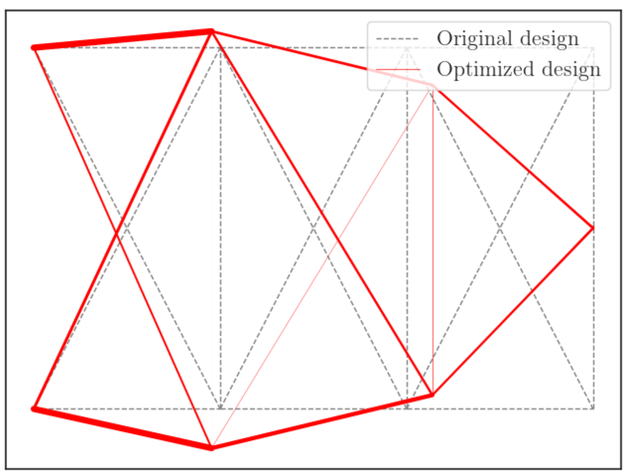

Figure 14: The final truss structure obtained by the double loop approach at 500th optimization iteration (Application2: Case 1).

4.3.2. Case 2: Multiple random loads

The last example is an extension of Case 1, to demonstrate the effectiveness of the proposed approach for RBDO under the case of multiple random loads. The truss structure is subjected to six Gaussian random loads, as shown in Figure 15. The loads independently follow the same distribution, with the mean value of 44.4822 kN and the coefficient of variation of 0.15. For the reliability analysis, the threshold of the compliance is taken as 500 ($\times 112.984$ kN $\cdot$ mm), and 300 representative points are adopted. Other settings are identical to those of Case 1.

Figure 16 shows the threshold of the operator norm evaluated with 50 samples of design vector. Table 6 presents the results of both the proposed approach and the double loop approach, with the maximum number of the calls to the reliability function being 2000. The results demonstrate the proposed approach achieves a superior design compared to the double loop approach, while significantly reducing computational costs. When the double loop approach reaches its maximum iteration number $N_{\mathrm{It}} = 500$, the objective function decreases to 93.055 ($\times$ 0.4536 kg), representing a 1.7 % improvement compared to the proposed approach (see Table 6). Nevertheless, this improvement comes at the expense of conducting 25000 reliability analyses. In this regard, the proposed approach offers a powerful way for structural design under uncertainty.

To provide a more comprehensive analysis of the proposed approach, it is further compared with the method recently introduced by Yang et al. (2022b), denoted as Gradient-based method 1. The method has been successfully extended to the reliability-based topology optimization (Yang et al., 2022a, 2024). It combines the globally convergent version of the method of moving asymptotes (GCMMA) (Svanberg, 2002) with a highly efficient strategy for sensitivity analysis. Although many recent studies on surrogate models can significantly reduce computational costs, they are outside the scope of this study and thus not included in the comparisons. Nonetheless, the proposed approach can be integrated with surrogate models to further reduce computational costs, for example, by incorporating surrogate models into the reliability analysis process or solving the deterministic optimization problems. The original RBDO problem is also solved by the GCMMA with the finite difference method for obtaining the gradient information, denoted as Gradient-based method 2. Both methods use the first feasible design found by the double loop approach adopted in this example as the initial solution. The algorithms are terminated if they fail to converge within 100 iterative steps. It should be noted that the GCMMA includes an inner loop at each optimization step to ensure the feasibility of intermediate solutions, which can increase the number of the reliability analyses. The corresponding optimization results are presented in Table 7. It is seen that Gradient-based method 1 demonstrates significantly better efficiency than Gradient-based method 2, which fails to converge in this example. But Gradient-based method 1 dose not achieve a solution as good as the proposed approach, partly due to the complex and irregular reliability contour surface. To illustrate this point, the sliced contour map of the reliability index in dimensions x_{18} and x_{21} (the vertical coordinates of nodes 2 and 6), with the other dimensions fixed, is plotted and shown in Figure 17. It is shown that the contour exhibits a high degree of non-linearity and that the reliability index is a non-bijective function of the design variables. From this sliced contour map, it can be inferred that the whole contour map of the reliability index is much more complex and irregular. Given this, the proposed approach can be advantageous in both computational efficiency and robustness. Furthermore, if the final solution of the proposed approach is used as the initial solution for Gradient-based method 1, a better solution is obtained, with an objective function value of value 92.640 ($\times$ 0.4536 kg) and 11558 function evaluations. This indicates that the proposed approach can effectively serve as a pre-optimizer for gradient-based optimization algorithms.

To evaluate the performance of the PDEM in the reliability assessment step, subset simulation (SS), Latin hypercube sampling (LHS), and MCS are also adopted to estimate the failure probability of the structure. In particular, the failure probability with different thresholds at the design found by the double loop approach (see Table 6) is calculated using the four methods, as shown in Figure 18. The PDEM uses 300 representative points, while MCS and LHS use 100000 and 1000 samples, respectively. For SS, the probability of the intermediate events is set to 0.1, with 400 samples employed at each stage, resulting in a total of 1120 samples to estimate the failure probability. As observed in Figure 18, both SS and the PDEM accord well with MCS, whereas LHS performs less accurately. In terms of efficiency, the PDEM requires fewer deterministic analyses but takes little time to solve the GDEE (less than 2 seconds). Although SS involves more deterministic analyses, the short computation time for the response analysis ensures that the overall efficiency remains high. Thus, in this example, both the PDEM and SS demonstrate satisfactory accuracy and efficiency. Based on this comparison, it is easy to infer the influences of the reliability analysis methods on the RBDO results, since the reliability analysis and optimization process are decoupled in the proposed approach.

To further examine the performance of the QPSO, the PSO and a gradient-based optimization algorithm, i.e., GCMMA, are employed to solve the decoupled deterministic optimization problem. For the QPSO and the PSO, the population size N_{p} and the maximum number of iteration N_{It} are set to 50 and 500, respectively. Given the stochastic nature of the QPSO and the PSO, each algorithm is run 10 times. For the GCMMA, the gradient information is obtained using the finite difference method, and the initial solution is the first feasible design found by the QPSO. The iteration histories, in terms of the average objective function value, obtained by the QPSO and the PSO are shown in Figure 19. The iteration history for the GCMMA are shown Figure 20. The final average objective function values for the QPSO and the PSO are 95.343 and 125.021 ($\times$ 0.4536 kg), respectively, while the final objective function value for the GCMMA is 94.510 ($\times$ 0.4536 kg). All the solutions are feasible. It is found that the QPSO demonstrates better global search capability and optimization performance compared to the PSO, which often shows premature convergence. The results of the gradient-based GCMMA are similar to those of the QPSO, with an acceptable difference in the objective function values. However, as previously analyzed, when the GCMMA is adopted to directly solve the original RBDO problem, the optimization results are not ideal. On the other hand, the QPSO performs well in handling both the original RBDO problem and the decoupled deterministic optimization problem. This also indicates that the decoupled deterministic optimization problem is easier to solve than the original RBDO problem.

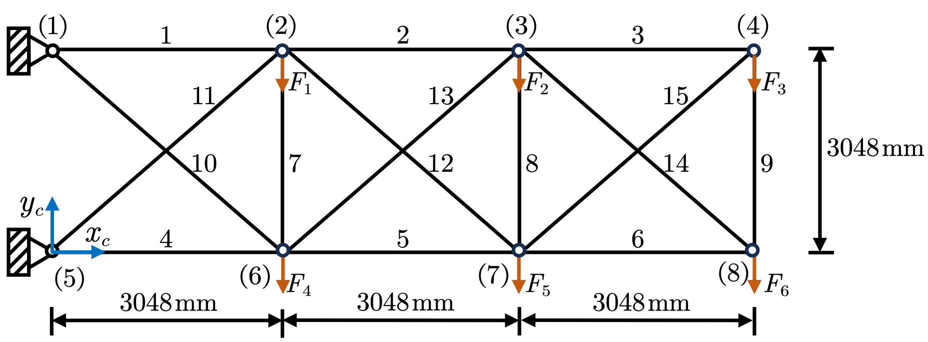

Figure 15: A 15-bar truss structure (Application 2: Case 2).

Table 6: The results obtained by different approaches (Application 2: Case 2).

Approach	Threshold	N_r	N_f	Objective function value	Operator norm	β
Double loop approach	β^{th} =2.34	2000	600000	101.590	0.919	2.366
Proposed approach	ON^{th} =0.823	50+1	40300	94.632	0.823	2.366

Note: (1) N_r and N_f denote the numbers of reliability analyses and function evaluations; (2) the unit of the objective function value is ($\times$ 0.4536 kg).

Table 7: The results obtained by the gradient-based RBDO methods (Application 2: Case 2).

Approach	N_r	N_f	Objective function value	Operator norm	β
Gradient-based method 1	101	33658	138.651	0.835	2.330
Gradient-based method 2	14676	4402800	198.234	0.553	Inf

Note: (1) N_r and N_f denote the numbers of reliability analyses and function evaluations; (2) the unit of the objective function value is ($\times$ 0.4536 kg).

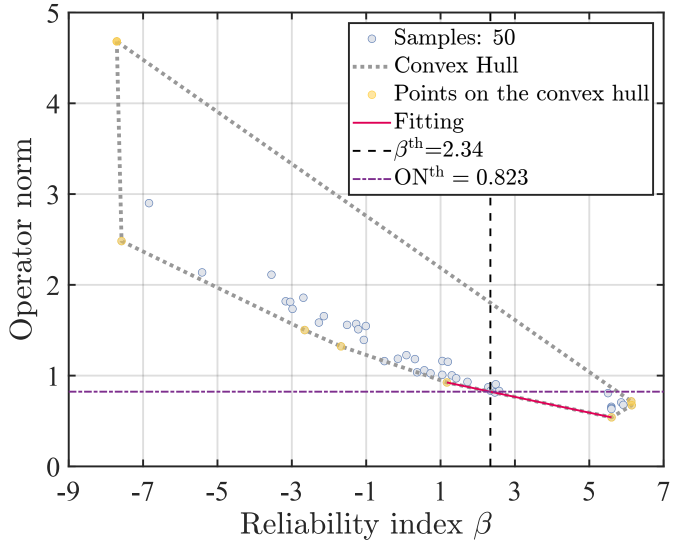

Figure 16: The evaluation of the threshold of the operator norm (Application2: Case 2).

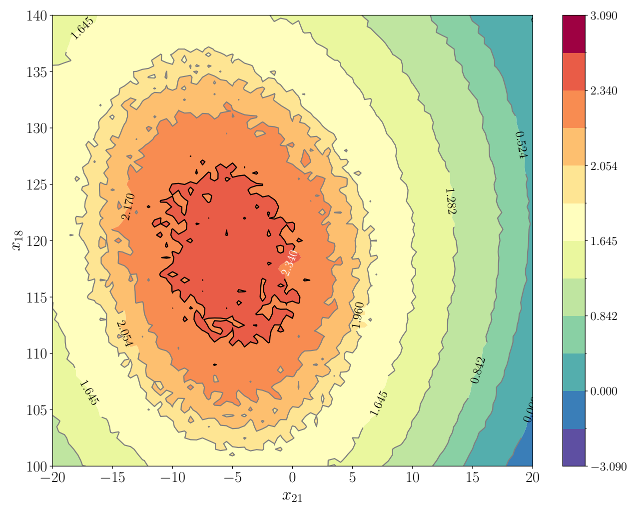

Figure 17: Sliced contour maps of the reliability index (Application 2: Case 2).

5. Conclusions

This contribution presents an approximate decoupled reliability-based design optimization approach for a specific class of RBDO problems concerning linear truss structures under random loads, with failure event defined by compliance. Grounded in the operator norm theory, this approach offers a potent and efficient means for design exploration with acceptable accuracy trade-offs. The key innovation lies in the application of the operator norm theory in terms of structural compliance. Based on it, the proposed approach transforms the RBDO problem into a deterministic optimization task through a limited number of reliability analyses, facilitated by the

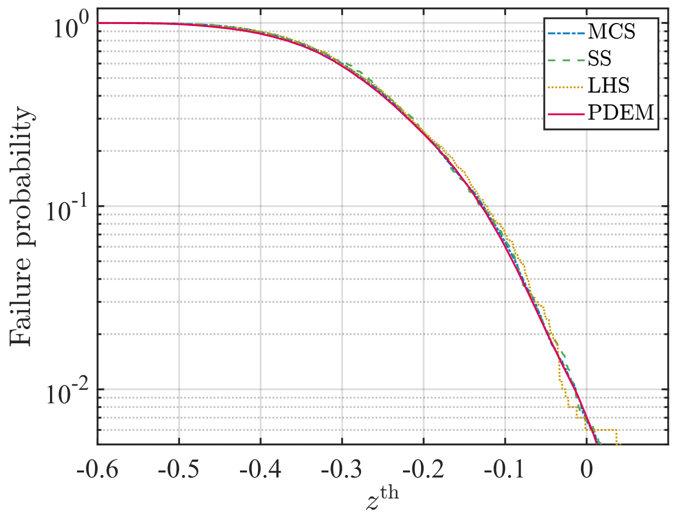

Figure 18: Probability failure curve obtained by different methods (Application 2: Case 2).

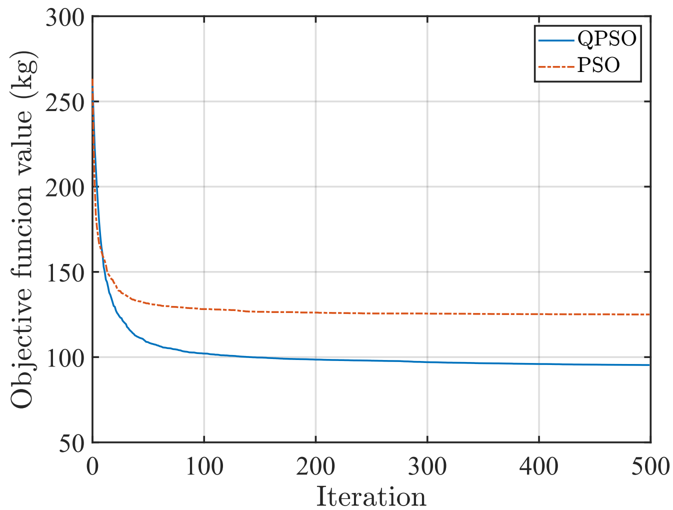

Figure 19: Iteration history in terms of the average objective function value obtained by the QPSO and the PSO (Application 2: Case 2).

probability density evolution method (PDEM). Once the deterministic optimization problem is formulated, the solution of the whole RBDO problem can be obtained without further reliability analysis, which results in a considerably improved computational efficiency. Numerical examples demonstrate that, with restrained computational resources, the proposed approach efficiently provides designs comparable to those obtained through the double loop technique. This contribution not only extends the frontier of the operator norm theory in the RBDO framework but also provides a valuable exploratory tool for decision-making in the early design phases of real-world engineering structures.

Future research efforts include finding more effective ways for determining the threshold of

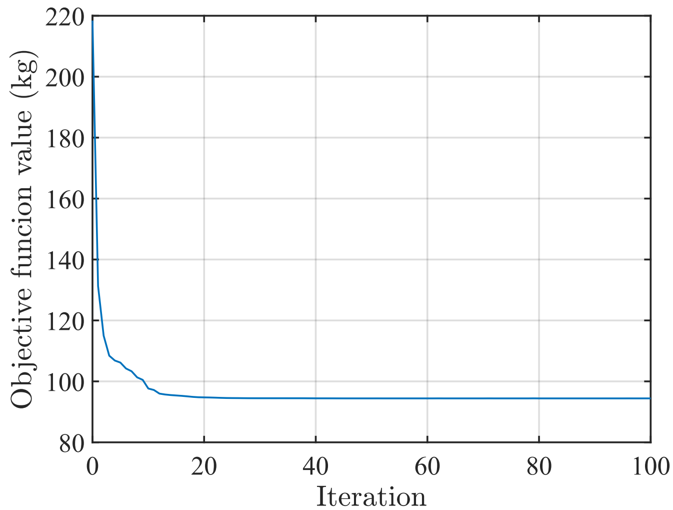

Figure 20: Iteration history in terms of the average objective function value obtained by the GCMMA (Application 2: Case 2).

the operator norm. Another direction for future research involves extending the approach to the reliability-based design optimization of dynamical systems.

6. Acknowledgments

Financial supports from the German Research Foundation (Deutsche Forschungsgemeinschaft, DFG) under Grant No. 527637016, the postdoctoral Research Fund of Shaanxi Province under Grant No. 2023BSHTBZZ39, and the National Natural Science Foundation of China under Grant No. 51725804 are highly appreciated. The first author appreciates the support of the International Exchange Program for Graduate Students, Tongji University (No. 2023020028) for her visit to TU Dortmund University.

7. Appendix: Numerical procedures for the PDEM

The numerical procedures for solving the GDEE (Eq.(24)) are as follows:

1. Discretize the probability-assigned space $\Omega_{\boldsymbol{\Theta}}$ with a representative point set $\mathcal{P}_{\text{sel}} = \{(\boldsymbol{\theta}_q, P_q)\}_{q=1}^{n_{\text{sel}}}$ based on the generalized F-discrepancy minimization-based point selection strategy (Chen et al., 2016a; Chen and Chan, 2019); n_{sel} is the number of the representative points; $\boldsymbol{\theta}_q = (\theta_{q1}, \cdots, \theta_{qn_\theta})^{\mathrm{T}}$ is qth representative point corresponding to the representative region

$\Omega_{\boldsymbol{\Theta}_q}$; and P_q is the assigned probability of $\boldsymbol{\theta}_q$ given by

$$P_q = \int_{\Omega_{\boldsymbol{\Theta}_q}} p_{\boldsymbol{\Theta}}(\boldsymbol{\theta})\,\mathrm{d}\boldsymbol{\theta}. \tag{33}$$

2. Perform deterministic structural analyses for the representative points $\boldsymbol{\theta}_q, q = 1, \cdots, n_{\mathrm{sel}}$, to evaluate the velocity responses $\dot{W}(\boldsymbol{\theta}_q, \tau; \boldsymbol{x}), q = 1, \cdots, n_{\mathrm{sel}}$.
3. Substitute each of the velocity responses $\dot{W}(\boldsymbol{\theta}_q, \tau; \boldsymbol{x}), q = 1, \cdots, n_{\mathrm{sel}}$, into the GDEE (Eq. (24)), and solve the GDEEs by the finite difference method (Li and Chen, 2009) to obtain the joint PDFs $p_{W\boldsymbol{\Theta}}(w, \boldsymbol{\theta}_q, \tau; \boldsymbol{x}), q = 1, \cdots, n_{\mathrm{sel}}$.
4. Synthesize the results of the GDEEs to obtain the PDF of the normalized compliance, namely

$$p_U(u; \boldsymbol{x}) = \int_{\Omega_{\boldsymbol{\Theta}}} p_{W\boldsymbol{\Theta}}(w, \boldsymbol{\theta}, \tau; \boldsymbol{x})\mathrm{d}\boldsymbol{\theta}\Big|_{w=u,\tau=\tau_c} = \sum_{q=1}^{n_{\mathrm{sel}}} p_{W\boldsymbol{\Theta}}(w, \boldsymbol{\theta}_q, \tau; \boldsymbol{x})\big|_{w=u,\tau=\tau_c}. \tag{34}$$

References

Agrawal, R.K., Kaur, B., Agarwal, P., 2021. Quantum inspired particle swarm optimization with guided exploration for function optimization. Applied Soft Computing 102, 107122. doi:10.1016/j.asoc.2021.107122.

Aoues, Y., Chateauneuf, A., 2010. Benchmark study of numerical methods for reliability-based design optimization. Structural and Multidisciplinary Optimization 41, 277–294. doi:10.1007/s00158-009-0412-2.

Au, S., Beck, J., 2001a. First excursion probabilities for linear systems by very efficient importance sampling. Probabilistic Engineering Mechanics 16, 193–207. doi:10.1016/S0266-8920(01)00002-9.

Au, S.K., Beck, J.L., 2001b. Estimation of small failure probabilities in high dimensions by subset simulation. Probabilistic Engineering Mechanics 16, 263–277. doi:10.1016/S0266-8920(01)00019-4.

Beck, A.T., Gomes, W.J.D.S., 2012. A comparison of deterministic, reliability-based and risk-based structural optimization under uncertainty. Probabilistic Engineering Mechanics 28, 18–29. doi:10.1016/j.probengmech.2011.08.007.

Bendsøe, M.P., Sigmund, O., 1999. Material interpolation schemes in topology optimization. Archive of Applied Mechanics 69, 635–654. doi:10.1007/s004190050248.

Canelas, A., Carrasco, M., López, J., 2024. Topology optimization of truss structures under failure probability using the Bernstein approximation. Computers & Structures 296, 107295. doi:10.1016/j.compstruc.2024.107295.

Cao, X.Y., Feng, D.C., Beer, M., 2023. Consistent seismic hazard and fragility analysis considering combined capacity-demand uncertainties via probability density evolution method. Structural Safety 103, 102330. doi:10.1016/j.strusafe.2023.102330.

Carlon, A.G., Lopez, R.H., Espath, L.F.R., Miguel, L.F.F., Beck, A.T., 2019. A stochastic gradient approach for the reliability maximization of passively controlled structures. Engineering Structures 186, 1–12. doi:10.1016/j.engstruct.2019.01.121.

Chen, J., Chan, J., 2019. Error estimate of point selection in uncertainty quantification of nonlinear structures involving multiple nonuniformly distributed parameters. International Journal for Numerical Methods in Engineering 118, 536–560. doi:10.1002/nme.6025.

Chen, J.B., Li, J., 2007. The extreme value distribution and dynamic reliability analysis of nonlinear structures with uncertain parameters. Structural Safety 29, 77–93. doi:10.1016/j.strusafe.2006.02.002.

Chen, J.B., Li, J., 2009. A note on the principle of preservation of probability and probability density evolution equation. Probabilistic Engineering Mechanics 24, 51–59. doi:10.1016/j.probengmech.2008.01.004.

Chen, J.B., Yang, J.S., Jensen, H.A., 2020. Structural optimization considering dynamic reliability constraints via probability density evolution method and change of probability measure. Structural and Multidisciplinary Optimization 62, 2499–2516. doi:10.1007/s00158-020-02621-4.

Chen, J.B., Yang, J.Y., Li, J., 2016a. A GF-discrepancy for point selection in stochastic seismic response analysis of structures with uncertain parameters. Structural Safety 59, 20–31. doi:10.1016/j.strusafe.2015.11.001.

Chen, N., Yu, D., Xia, B., Ma, Z., 2016b. Topology optimization of structures with interval random parameters. Computer Methods in Applied Mechanics and Engineering 307, 300–315. doi:10.1016/j.cma.2016.03.036.

Cheng, G.D., Xu, L., Jiang, L., 2006. A sequential approximate programming strategy for reliability-based structural optimization. Computers & Structures 84, 1353–1367. doi:10.1016/j.compstruc.2006.03.006.

Du, X.P., Chen, W., 2004. Sequential optimization and reliability assessment method for efficient probabilistic design. Journal of Mechanical Design 126, 225–233. doi:10.1115/1.1649968.

Faes, M.G., Valdebenito, M.A., 2020. Fully decoupled reliability-based design optimization of structural systems subject to uncertain loads. Computer Methods in Applied Mechanics and Engineering 371, 113313. doi:10.1016/j.cma.2020.113313.

Faes, M.G.R., Valdebenito, M.A., 2021. Fully decoupled reliability-based optimization of linear structures subject to Gaussian dynamic loading considering discrete design variables. Mechanical Systems and Signal Processing 156, 107616. doi:10.1016/j.ymssp.2021.107616.

Faes, M.G.R., Valdebenito, M.A., Moens, D., Beer, M., 2020. Bounding the first excursion probability of linear structures subjected to imprecise stochastic loading. Computers & Structures 239, 106320. doi:10.1016/j.compstruc.2020.106320.

Faes, M.G.R., Valdebenito, M.A., Moens, D., Beer, M., 2021. Operator norm theory as an efficient tool to propagate hybrid uncertainties and calculate imprecise probabilities. Mechanical Systems and Signal Processing 152, 107482. doi:10.1016/j.ymssp.2020.107482.

Ho-Huu, V., Nguyen-Thoi, T., Nguyen-Thoi, M.H., Le-Anh, L., 2015. An improved constrained differential evolution using discrete variables (D-ICDE) for layout optimization of truss structures. Expert Systems with Applications 42, 7057–7069. doi:10.1016/j.eswa.2015.04.072.

Huang, X., Xie, Y.M., 2010. Evolutionary Topology Optimization of Continuum Structures: Methods and Applications. Wiley, Chichester, West Sussex.

Jensen, H.A., Jerez, D.J., Valdebenito, M., 2020. An adaptive scheme for reliability-based global design optimization: a markov chain Monte Carlo approach. Mechanical Systems and Signal Processing 143, 106836. doi:10.1016/j.ymssp.2020.106836.

Jensen, H.A., Valdebenito, M.A., Schuëller, G.I., Kusanovic, D.S., 2009. Reliability-based optimization of stochastic systems using line search. Computer Methods in Applied Mechanics and Engineering 198, 3915–3924. doi:10.1016/j.cma.2009.08.016.

Jerez, D.J., Fragkoulis, V.C., Ni, P., Mitseas, I.P., Valdebenito, M.A., Faes, M.G.R., Beer, M., 2024. Operator norm-based determination of failure probability of nonlinear oscillators with fractional derivative elements subject to imprecise stationary Gaussian loads. Mechanical Systems and Signal Processing 208, 111043. doi:10.1016/j.ymssp.2023.111043.

Jiang, Y., Zhang, X., Beer, M., Zhou, H., Leng, Y., 2024. An efficient method for reliability-based design optimization of structures under random excitation by mapping between reliability and operator norm. Reliability Engineering & System Safety 245, 109972. doi:10.1016/j.ress.2024.109972.

Kennedy, J., Eberhart, R., 1995. Particle swarm optimization, in: Proceedings of ICNN'95 - International Conference on Neural Networks, IEEE. pp. 1942–1948. doi:10.1109/icnn.1995.488968.

Kuschel, N., Rackwitz, R., 1997. Two basic problems in reliability-based structural optimization. Mathematical Methods of Operations Research 46, 309–333. doi:10.1007/BF01194859.

Li, G., Yang, H., Zhao, G., 2020. A new efficient decoupled reliability-based design optimization method with quantiles. Structural and Multidisciplinary Optimization 61, 635–647. doi:10.1007/s00158-019-02384-7.

Li, J., Chen, J.B., 2005. Dynamic response and reliability analysis of structures with uncertain parameters. International Journal for Numerical Methods in Engineering 62, 289–315. doi:10.1002/nme.1204.

Li, J., Chen, J.B., 2008. The principle of preservation of probability and the generalized density evolution equation. Structural Safety 30, 65–77. doi:10.1016/j.strusafe.2006.08.001.

Li, J., Chen, J.B., 2009. Stochastic Dynamics of Structures. John Wiley & Sons (Asia) Pte Ltd, Singapore.

Li, X.L., Meng, Z., Chen, G.H., Yang, D.X., 2019. A hybrid self-adjusted single-loop approach for reliability-based design optimization. Structural and Multidisciplinary Optimization 60, 1867–1885. doi:10.1007/s00158-019-02291-x.

Liang, J.H., Mourelatos, Z.P., Nikolaidis, E., 2007. A single-loop approach for system reliability-based design optimization. Journal of Mechanical Design 129, 1215–1224. doi:10.1115/DETC2006-99240.

Meng, Z., Li, G., Wang, X., Sait, S.M., Yıldız, A.R., 2020. A comparative study of metaheuristic algorithms for reliability-based design optimization problems. Archives of Computational Methods in Engineering 28, 1853–1869. doi:10.1007/s11831-020-09443-z.

Moustapha, M., Sudret, B., 2019. Surrogate-assisted reliability-based design optimization: a survey and a unified modular framework. Structural and Multidisciplinary Optimization 60, 2157–2176. doi:10.1007/s00158-019-02290-y.

Muscolino, G., Santoro, R., Sofi, A., 2016. Reliability analysis of structures with interval uncertainties under stationary stochastic excitations. Computer Methods in Applied Mechanics and Engineering 300, 47–69. doi:10.1016/j.cma.2015.10.023.

Ni, P., Jerez, D.J., Fragkoulis, V.C., Faes, M.G.R., Valdebenito, M.A., Beer, M., 2022. Operator norm-based statistical linearization to bound the first excursion probability of nonlinear structures subjected to imprecise stochastic loading. ASCE-ASME Journal of Risk and Uncertainty in Engineering Systems, Part A: Civil Engineering 8, 04021086. doi:10.1061/AJRUA6.0001217.

Papadrakakis, M., Lagaros, N.D., 2002. Reliability-based structural optimization using neural networks and Monte Carlo simulation. Computer Methods in Applied Mechanics and Engineering 191, 3491–3507. doi:10.1016/S0045-7825(02)00287-6.

dos Santos Coelho, L., 2010. Gaussian quantum-behaved particle swarm optimization approaches for constrained engineering design problems. Expert Systems with Applications 37, 1676–1683. doi:10.1016/j.eswa.2009.06.044.

Schuëller, G.I., Jensen, H.A., 2008. Computational methods in optimization considering uncertainties - an overview. Computer Methods in Applied Mechanics and Engineering 198, 2–13. doi:10.1016/j.cma.2008.05.004.

Sun, J., Fang, W., Wu, X.J., Palade, V., Xu, W.B., 2012. Quantum-behaved particle swarm optimization: analysis of individual particle behavior and parameter selection. Evolutionary Computation 20, 349–393. doi:10.1162/evco_a_00049.

Sun, J., Feng, B., Xu, W.B., 2004. Particle swarm optimization with particles having quantum behavior, in: Proceedings of the 2004 Congress on Evolutionary Computation, pp. 325–331. doi:10.1109/cec.2004.1330875.

Svanberg, K., 2002. A class of globally convergent optimization methods based on conservative convex separable approximations. SIAM Journal on Optimization 12, 555–573. doi:10.1137/S1052623499362822.

Tropp, J., 2004. Topics in Sparse Approximation. Ph.D. thesis. The University of Texas at Austin.

Valdebenito, M.A., Schuëller, G.I., 2010. A survey on approaches for reliability-based optimization. Structural and Multidisciplinary Optimization 42, 645–663. doi:10.1007/s00158-010-0518-6.

Weng, L.L., Yang, J.S., Chen, J.B., Beer, M., 2023. Structural design optimization under dynamic reliability constraints based on probability density evolution method and quantum-inspired optimization algorithm. Probabilistic Engineering Mechanics 74, 103494. doi:10.1016/j.probengmech.2023.103494.

Yang, J.S., Chen, J.B., Beer, M., 2024. Seismic topology optimization considering first-passage probability by incorporating probability density evolution method and bi-directional evolutionary structural optimization. Engineering Structures 314, 118382. doi:10.1016/j.engstruct.2024.118382.

Yang, J.S., Chen, J.B., Beer, M., Jensen, H.A., 2022a. An efficient approach for dynamic-reliability-based topology optimization of braced frame structures with probability density evolution method. Advances in Engineering Software 173, 103196. doi:10.1016/j.advengsoft.2022.103196.

Yang, J.S., Chen, J.B., Jensen, H.A., 2022b. Structural design optimization under dynamic reliability constraints based on the probability density evolution method and highly-efficient sensitivity analysis. Probabilistic Engineering Mechanics 68, 103205. doi:10.1016/j.probengmech.2022.103205.

Yang, J.S., Jensen, H.A., Chen, J.B., 2022c. Structural optimization under dynamic reliability constraints utilizing probability density evolution method and metamodels in augmented input space. Structural and Multidisciplinary Optimization 65, 107. doi:10.1007/s00158-022-03188-y.